



LAWRENCE
LIVERMORE
NATIONAL
LABORATORY

A Generalized Fast Frequency Sweep Algorithm for Coupled Circuit-EM Simulations

G. Ouyang , V. Jandhyala, N. Champagne, R. Sharpe, B. J. Fasenfest, J. D. Rockway

December 15, 2004

Disclaimer

This document was prepared as an account of work sponsored by an agency of the United States Government. Neither the United States Government nor the University of California nor any of their employees, makes any warranty, express or implied, or assumes any legal liability or responsibility for the accuracy, completeness, or usefulness of any information, apparatus, product, or process disclosed, or represents that its use would not infringe privately owned rights. Reference herein to any specific commercial product, process, or service by trade name, trademark, manufacturer, or otherwise, does not necessarily constitute or imply its endorsement, recommendation, or favoring by the United States Government or the University of California. The views and opinions of authors expressed herein do not necessarily state or reflect those of the United States Government or the University of California, and shall not be used for advertising or product endorsement purposes.

This work was performed under the auspices of the U.S. Department of Energy by University of California, Lawrence Livermore National Laboratory under Contract W-7405-Eng-48.

Table of Contents

1.	Abstract	
2.	Introduction	3
3.	Single Point AWE Surface Impedance Pade Expansion Formulation	3
4.	Plane Wave Correction and Multiple Excitation Vectors	8
5.	Automated Multipoint Fast Frequency Sweep	9
6.	Other Integral Equations	11
	PMCHWT	11
	MFIE / CFIE	12
	Coupled Circuit-EM Formulations: Contacts and Coupled System Matrix	12
	Coupled Circuit-EM Formulations: N-port representation	15
	Lumped Loads	15
7.	Results	16
	PEC Dipole in free space with delta-gap source	17
	Conducting Dipole in free space with delta-gap source	19
	Dielectric Cube	19
	Lumped Load Test	20
	Resistive Interconnect	22
8.	Conclusion	23
9.	References	23

1. Abstract

An Asymptotic Wave Expansion (AWE) technique is implemented into the EIGER computational electromagnetics code. The AWE fast frequency sweep is formed by separating the components of the integral equations by frequency dependence, then using this information to find a rational function approximation of the results. The standard AWE method is generalized to work for several integral equations, including the EFIE for conductors and the PMCHWT for dielectrics. The method is also expanded to work for two types of coupled circuit-EM problems as well as lumped load circuit elements. After a simple bisecting adaptive sweep algorithm is developed, dramatic speed improvements are seen for several example problems.

2. Introduction

Frequency domain techniques are popular for analyzing electromagnetics and coupled circuit-EM problems. These techniques, such as the method of moments (MoM) and the finite element method (FEM), are used to determine the response of an antenna or other device in the sinusoidal steady state at a single frequency. Because only one frequency is solved at a time, it may take a long time to calculate the parameters for wideband devices. It is also a demanding task to calculate enough frequency points to perform an inverse Fourier transform to get the time domain response of the system.

Several techniques have been used to perform fast frequency sweeps, many of which are based on forming a Pade approximation to the system. The Pade approximation, which is a rational function adaptation of the Taylor series, is first created for a single frequency expansion point. The Pade function is then used to approximate the response of the system for frequencies around the expansion point. For very wideband simulations, more than one expansion point may be used. The Asymptotic Wave Expansion (AWE) method is one common technique for forming the Pade approximation. It was first demonstrated in lumped-load circuit simulations, but has recently been shown to be effective at quasi-static and full wave simulations at low frequencies. The AWE technique was successfully used for quasi-static-circuit simulations in [1].

Recently, the AWE technique was implemented in EIGER, a frequency-domain code capable of MoM, FEM, and coupled MoM/FEM simulations. It contains several Green's functions, including those for homogeneous regions, layered material, and periodic structures. It also has the ability to solve coupled circuit-EM problems by solving a combined system matrix or by finding a port representation of the EM section of a simulation.

The AWE formulation implemented in EIGER is based upon the separation of the system matrix into several sub-matrices with similar frequency content. This may be done without much additional processor time if the different types of potentials are assembled into separate matrices rather than one unified system matrix. Since each potential often has an explicit frequency dependence attached to it, this explicit frequency dependence is removed and used to determine which submatrix should contain each particular potential. Note that the method does not account for frequency variation due to inter-element phasing from the Green's function. Therefore, the AWE technique works best at lower frequencies where the inter-element phasing does not dominate.

The solution for each unknown and its derivatives are calculated from the frequency dependent submatrices. These derivatives are used to form the Pade rational function approximation, which is used to find the approximation for other frequencies. [2] When multiple excitation groups are used, several Pade functions are formed, one for each excitation group.

3. Single Point AWE Surface Impedance Pade Expansion Formulation

A single point AWE expansion is used to solve for the unknowns and their derivatives with respect to frequency at a single frequency point. The derivatives in a Pade rational function approximation are employed to extrapolate the results for arbitrary nearby frequencies. In practice, the bandwidth from a single frequency expansion varies depending on the amount of allowable error and the geometry of the structure. For many wideband solutions, or in cases where the error tolerance is very low, several AWE expansion points must be chosen. However, for simplicity, the case of a single AWE expansion point will be discussed here and the multipoint extension will be discussed later.

The Electric Field Integral Equation (EFIE) is used to obtain the basic AWE expansion for a perfect electric conductor (PEC). The mixed potential formulation for the EFIE is given by

$$j\omega\mathbf{A} + \nabla\Phi = -\mathbf{E}^i, \quad (1)$$

where \mathbf{A} is the magnetic vector potential, Φ is the electric scalar potential, \mathbf{E}^i is the impressed electric field, and ω is the radian frequency. In supermatrix form, the equation is

$$[Z] [X] = [Y]. \quad (2)$$

where Z is the system matrix, X is the unknown vector, and Y is the forcing function, in this case the incident field. To perform AWE, the system matrix is separated with respect to frequency content as

$$\left[\frac{B_0}{s} + B_1 + sB_2 \right] [X] = [Y], \quad (3)$$

where $s = j\omega$. In the case of the EFIE, the B_0 component comes from the scalar potential, the B_2 component comes from the vector potential, and the B_1 matrix is actually empty or zero. Each of the B components is placed into its own separate matrix. Note that this expansion ignores the frequency dependence due to phasing between elements and only accounts for the explicit frequency dependence in front of each term. For this reason, it is more effective for quasi-static Green's functions, where the phase term is neglected, or for electrically small structures, where the inter-element phasing is not significant. The implementation in EIGER uses the full-wave Green's function. For that reason error metrics appear slightly worse than for codes using a quasi-static Green's function.

When a surface impedance formulation is used, the governing equation becomes

$$j\omega\mathbf{A} + \nabla\Phi + Z_s\mathbf{J}_s = -\mathbf{E}^i, \quad (4)$$

where the surface impedance term Z_s has a $\sqrt{\omega}$ -type frequency dependence. This extra frequency dependence requires a different expansion term, $g = \sqrt{j\omega}$, and the expansion of the A matrix into more sub matrices as

$$\left[\frac{B_0}{g} + B_1 + \sqrt{g}B_2 + gB_3 \right] [X] = [Y], \quad (5)$$

where now the matrix B_0 contains the scalar potential term, B_1 is empty or zero, B_2 is sparse and contains only the self terms used in the surface impedance formulation, and B_3 contains the vector potential terms. This expansion around g is convenient because it allows for the surface impedance formulation. However, it does require more memory due to the added matrix.

After the system matrices have been filled, a k -moment AWE is performed around $g = g_0$. To perform the AWE, the first k -derivatives of the unknowns will be used to form the Taylor series approximation. The frequency is assumed to be such that $g = g_0 + \sigma$, where g_0 is $\sqrt{j\omega_0}$ (ω_0 is the expansion frequency) and σ is the scaled difference between the expansion frequency and the desired approximation frequency. The equation for the AWE is

$$(A_0 + \sigma A_1 + \sigma^2 A_2 + \sigma^3 A_3 + \sigma^4 A_4) (X_0 + \xi \sigma X_1 + (\xi \sigma)^2 X_2 + \dots + (\xi \sigma)^k X_k) \cong (Y_0 + \sigma Y_1 + \sigma^2 Y_2). \quad (6)$$

Here, ξ is a scaling factor that is used to improve conditioning when finding the Pade coefficients. The equation simply states that the Taylor series expansion of the system matrix times the Taylor series expansion of the unknowns needs to be approximately equal to the Taylor series expansion of the excitation vector. The A and Y matrices are the Taylor series coefficients from taking multiple derivatives with respect to g . The X vectors are the Taylor series coefficients for the unknown currents.

The A matrices can be found from the B matrices as

$$\begin{aligned} A_0 &= B_0 + g_0^2 B_1 + g_0^3 B_2 + g_0^4 B_3, \\ A_1 &= 2g_0 B_1 + 3g_0^2 B_2 + 4g_0^3 B_3, \\ A_2 &= B_1 + 3g_0 B_2 + 6g_0^2 B_3, \\ A_3 &= B_2 + 4g_0 B_3, \quad \text{and} \\ A_4 &= B_3. \end{aligned} \quad (7)$$

If the excitation vector is assumed to be frequency independent, the Y vectors are given by

$$\begin{aligned} Y_0 &= g_0^2 Z, \\ Y_1 &= 2g_0 Z, \quad \text{and} \\ Y_2 &= Z. \end{aligned} \quad (8)$$

If the excitation vector varies with frequency, as is the case with the phasing due to an incident plane wave, a different method that incorporates the actual first and second derivatives of the excitation vector should be used. One way to do this is discussed later.

Once the A and Y matrices are formed, they are used to find the X vectors in a recursive manner by equating like powers of σ . The X s can be found by solving the equations:

$$\begin{aligned}
A_0 X_0 &= Y_0 \\
A_0 X_1 &= \frac{Y_1 - A_1 X_0}{\xi} \\
A_0 X_2 &= \frac{Y_2}{\xi^2} - \frac{A_1 X_1}{\xi} - \frac{A_2 X_0}{\xi^2} \\
A_0 X_3 &= -\frac{A_1 X_2}{\xi} - \frac{A_2 X_1}{\xi^2} - \frac{A_3 X_0}{\xi^3}, \quad \text{and} \\
A_0 X_n &= -\frac{A_1 X_{n-1}}{\xi} - \frac{A_2 X_{n-2}}{\xi^2} - \frac{A_3 X_{n-3}}{\xi^3} - \frac{A_4 X_{n-4}}{\xi^4}, \quad n = 4 \dots k.
\end{aligned} \tag{9}$$

Since the problem of solving for the X vectors is a multiple right hand side problem, it is typically more efficient to find the LU factorization of A_0 once, then use that to solve for each X , rather than using an iterative solver. Overall, this solution should be $O(N^3)$ due to the LU factorization, while each of the matvecs and back substitutions are $O(N^2)$.

A fast frequency sweep could stop after the X vectors are determined, solving for each approximation frequency using the X vectors in a Taylor series approximation. Such an approximation for the i th unknown is given by

$$\tilde{X}_i = \overline{X_{i,k} \tau_k}, \quad \overline{\tau_k} = \begin{bmatrix} 1 \\ \tau \\ \tau^2 \\ \vdots \\ \tau^{k-1} \end{bmatrix} \quad \text{and} \quad \tau = \xi \sigma. \tag{10}$$

Equation (10) shows how individual unknowns can be solved across a broad frequency range without solving for all the unknowns. After the system has been solved at the expansion point, only the unknowns of interest need to be computed at the other frequencies.

If the Taylor coefficients are used to form a Pade approximation, the approximate solution may be more likely to converge near resonances. [2] Because the Pade approximation is a rational function, it can more closely match resonant behavior than a truncated power series. Typically L is used for the number of zeroes and M is the number of poles in the rational function. The Pade approximation is then given by

$$\tilde{X}_{i,Pade} = [L / M] = \frac{a_0 + a_1 \tau + a_2 \tau^2 + \dots + a_L \tau^L}{1 + b_1 \tau + b_2 \tau^2 + \dots + b_M \tau^M} \tag{11}$$

or

$$\tilde{x}_{i, Pade} = [L / M] = \frac{(\bar{L} \bar{\tau}_{L+1})}{(\bar{M} \bar{\tau}_{M+1})} \quad (12)$$

where the τ vector is a truncated top section of the τ vector in (10) and the L and M vectors contain the a and b coefficients.

The most time consuming part of forming the Pade approximation is to find both the numerator and denominator coefficients. The denominator coefficients (b) are found by solving the Hankel matrix

$$\begin{bmatrix} x_{L-M+1} & x_{L-M+2} & x_{L-M+3} & \cdots & x_L \\ x_{L-M+2} & x_{L-M+3} & & & x_{L+1} \\ x_{L-M+3} & x_{L-M+4} & & & x_{L+2} \\ \vdots & & & & \vdots \\ x_L & x_{L+1} & x_{L+2} & \cdots & x_{L+M+1} \end{bmatrix} \begin{bmatrix} b_M \\ b_{M-1} \\ b_{M-2} \\ \vdots \\ b_1 \end{bmatrix} = - \begin{bmatrix} x_{L+1} \\ x_{L+2} \\ x_{L+3} \\ \vdots \\ x_{L+M} \end{bmatrix} \quad (13)$$

for each unknown. [3] This is not terribly time consuming because the matrix is only $M \times M$ and M is typically around 7 or 8, so the solution may be found fairly cheaply using direct methods. As for the Tailor series approximation, if it is known ahead of time that only the results for certain unknowns are needed, then not all of the L and M vectors have to be created, further cutting solution time.

Unfortunately, the denominator coefficient matrix can often be poorly conditioned, reducing the accuracy of the final solution. One method which has been used to improve its conditioning is the ξ scaling factor shown in this formulation. This scaling factor can be chosen such that all the X s are roughly the same magnitude, which improves the conditioning of the denominator matrix. There are at least three methods previously used to choose ξ . All the methods rely on calculating at least some of the X vectors with an initial guess for ξ , then refining the value of ξ and re-calculating all the X vectors. The initial guess for ξ is typically chosen to be $\xi = (g_0)^{-1}$. Three of the methods are to choose are the following [1],[4]:

1. $\xi = \frac{|X_0|}{|X_1|}$,
2. $\xi = \left(\frac{|X_0|}{|X_{L+M-1}|} \right)^{\frac{1}{L+M-1}}$, or
3. $\xi = \xi \text{ mean} \left(\frac{|X_0|}{|X_1|} \right)$, where the division is performed element-wise.

Method three is currently implemented for several reasons. First, it requires only the computation of the first two x vectors before finding ξ , and second because it does not require a distinct ξ to be found for each unknown. This method seems to work for practical problems when $[L/M]$ is around [7/8]. [5]

Once the denominator coefficients have been found, the numerator coefficients can be solved from the recursive relation

$$\begin{aligned}
a_0 &= X_0, \\
a_1 &= X_1 + b_1 X_0, \\
a_2 &= X_1 + b_1 X_1 + b_2 X_0, \text{ and} \\
a_L &= X_L + \sum_{i=1}^{\min(L,M)} b_i X_{L-i}.
\end{aligned} \tag{14}$$

After the Pade approximations have been formed, the algorithm loops over the frequencies to find the fast solution. The approximation is found using equation (2) at each frequency. If an error metric is needed, the exact solution can be solved and compared to the AWE solution for each frequency.

4. Plane Wave Correction and Multiple Excitation Vectors

An important part of an accurate AWE solution is approximating the derivatives of the excitation vector correctly. The excitation can be considered constant for many types of excitations. In these cases, the associated Y vectors are

$$\begin{aligned}
Y_0 &= g_0^2 \bar{z}, \\
Y_1 &= 2g_0 \bar{z}, \text{ and} \\
Y_2 &= \bar{z},
\end{aligned} \tag{15}$$

where the z vector is the standard excitation vector filled normally. Frequency independent excitation vectors result from delta-gap voltage sources and sinusoidal circuit excitations.

Plane wave illumination, a common way to excite problems, does not create a frequency independent excitation vector. The phase on a plane wave excitation is

$$V_0 = e^{jk\hat{\mathbf{k}}\cdot\mathbf{r}_0} = e^{j\omega\sqrt{\mu\epsilon}\hat{\mathbf{k}}\cdot\mathbf{r}_0} \tag{16}$$

where $\hat{\mathbf{k}}$ is the direction of the incident plane wave and \mathbf{r}_0 is the vector from the origin to the observation point on an element. This phase clearly has a frequency dependence when the two vectors are not parallel. While this phase shift can be ignored, it results in a decreased accuracy for the AWE solution [3].

One method for correcting for the plane wave phase shift is to take the first two analytic derivatives of the plane wave phase and use them to fill the Y_1 and Y_2 vectors. A more complete method would be to take k -derivatives to match to all the AWE moments. However, using only the first two derivatives has the practical affect of halving the error norm and does not require storing any additional vectors.

The derivatives actually need to be taken on $yc_0 = g^2 V_0$, which is the phase coefficient used to generate the right-hand side for AWE. First, the phase is expressed with respect to $g = \sqrt{j\omega}$, as

$$V_0 = e^{g^2\sqrt{\mu\epsilon}\hat{\mathbf{k}}\cdot\mathbf{r}_0} = e^{g^2\phi}. \tag{17}$$

Next, the product rule is applied to find the first two derivatives of yc_0 :

$$\begin{aligned} yc_0 &= g^2 V_0, \\ yc_1 &= (2g + 2g^3 \phi) V_0, \quad \text{and} \\ yc_2 &= (4\phi^2 g^4 + 10\phi g^2 + 2) V_0. \end{aligned} \tag{18}$$

These equations for the y vectors can be used to increase the accuracy of AWE solutions with plane wave excitations.

Using multiple excitation groups for the same problem can be a useful technique. For instance, if the monostatic radar cross section is desired at several different angles at the same frequency, the impedance matrix can be filled once and then solved with different excitation vectors representing each of the directions of the incoming plane waves.

Implementing multiple excitation groups in AWE is fairly straightforward. Separate right hand side vectors Y_0 through Y_2 are formed for each excitation group and a different set of X moments are created. From these moments, a Pade approximation for each unknown with each excitation group is formed. This causes the amount of memory needed for the expansion frequency to increase by approximately $(3+k)(N)(\#excitation\ groups)$, where N is the number of unknowns in the problem. This memory increase is still much more efficient than refilling the impedance matrix for each excitation group which is what is necessary without multiple excitation groups.

5. Automated Multipoint Fast Frequency Sweep

In many cases a single frequency expansion point cannot be used to accurately calculate the approximations over the entire frequency range of interest, requiring a multipoint expansion. Several frequency expansion points are used, and the AWE method is applied to each one independently. Each expansion point is used to form the approximations for frequencies within a certain range of its center frequency. This multipoint method allows for a tradeoff between accuracy and efficiency. [6] The fewer expansion points used, the quicker the solution and the lower the accuracy.

An automated method of choosing the center frequencies is necessary to reduce user input and to help ensure bounds on error. User input expansion frequencies can lead to either over-resolution or to unacceptable error. An automated method that assigns expansion points and tests their accuracy bandwidth is a better solution.

The method implemented in EIGER relies on a binary bisection method to choose the expansion points. The first expansion point is chosen in the middle of the desired bandwidth. The approximation from this expansion is tested against the exact solution at the endpoints of the bandwidth. If the AWE solution at the highest or lowest frequency has too much error, the interval between the expansion point and the endpoint is split and another expansion point placed between the two frequencies. This process is repeated until the error in the approximation from each expansion point at the endpoints of the expansion point is within a specified tolerance. Once the expansion points are selected and solved, the approximations for all frequencies can be found by first finding the expansion point which is responsible for the frequency, then using the Pade approximation from that expansion point to calculate the approximate value.

Figure 1 shows a graphical representation of this scheme. The entire frequency range is shown as the black line. Every circle is a frequency that is solved exactly. The colored dotted lines show which expansion points are used to produce the approximation for a given frequency range. In this example, the first frequency expansion point (Exp. 1) is chosen in the center of the range. Since its approximation for the endpoints is not precise enough, both the top and bottom half are expanded around another point (Exp. 2 and Exp. 3). The bottom half error is now acceptable and Exp. 2 is used to find the approximation for all the frequencies in the lower half. The upper half error is still not good enough, so the band is further divided into Exp. 4 and Exp. 5. The error for Exp. 4 is now tested against the exact solution at Exp. 1 and Exp. 3, and found to be acceptable. The error for Exp. 5 at its endpoints is also acceptable, so the two are assigned half of the upper part of the frequency range.

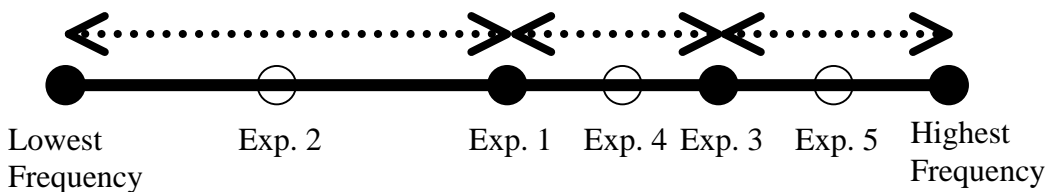


Figure 1. An example of the frequency expansion point distribution and the range of frequencies approximated by each point.

This method offers several strong advantages. First, the error at the endpoints can be controlled. While the error at the endpoints is not always the greatest error in a range, it usually is. Because testing is only done at the endpoints, there is low overhead for the testing. The exact solution at each expansion point is calculated during the AWE as the x_0 vector. In addition, this scheme can be implemented easily using a recursive technique and a tree data structure to hold the expansion points and their AWE data. This tree structure is shown in Figure 2.

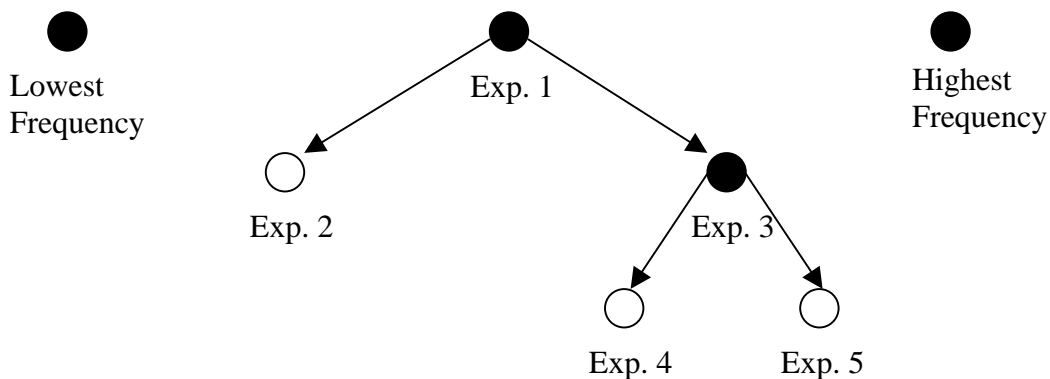


Figure 2. The tree structure used to create and store the data from the frequency expansion points.

This technique can be further improved. From Figure 1, it is clear that some expansion points are never used to find approximations even for frequencies near them. This algorithm is

wasteful of the computational cost used to solve at these frequencies. A more efficient algorithm is shown in Figure 3.

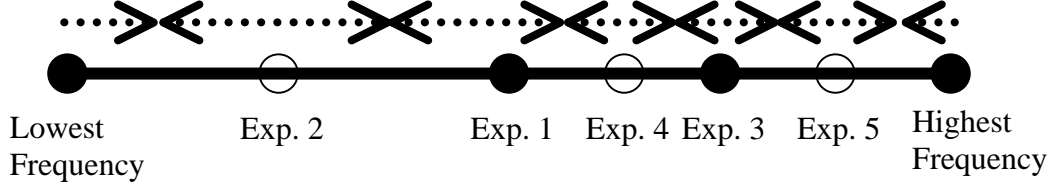


Figure 3. A more efficient allocation of frequencies.

Here every point that is solved exactly is assigned a region. This should result in a lower error overall. However, the exact point where a frequency should be controlled by one expansion point or another is less clear. In Figure 1, each expansion point was used to the endpoints at which had proven to be accurate. For Figure 2, some of the expansion points aren't used as far from their center as they could be and other expansion points haven't proven their accuracy out to the end of their range. While the error is less rigorously controlled, it should be lower in general as error tends to increase away from an expansion point unless there is a strong nearby resonance. The first scheme is the one currently implemented in EIGER. However, it would be fairly easy to implement the second one later if desired.

6. Other Integral Equations

The Pade approximation need not be limited to conductors in free space. It may be applied to any formulation where the operators may be separated by frequency type. Once the frequency behavior of each operator is determined, it can be placed into one of the B matrices.

PMCHWT

For the PMCHWT formulation, the equations for the electric and magnetic potentials are

$$\begin{aligned} \mathbf{E}(\mathbf{J}, \mathbf{M}) &= -j\omega\mathbf{A}(\mathbf{J}) - \nabla\Phi(\mathbf{J}) - \frac{1}{\epsilon}\nabla\times\mathbf{F}(\mathbf{M}) \quad \text{and} \\ \mathbf{H}(\mathbf{J}, \mathbf{M}) &= -j\omega\mathbf{F}(\mathbf{M}) - \nabla\Psi(\mathbf{M}) + \frac{1}{\mu}\nabla\times\mathbf{A}(\mathbf{J}). \end{aligned} \tag{19}$$

Both the vector potentials \mathbf{A} and \mathbf{F} need to be filled into the B_3 matrix, while the scalar potentials have a f^{-1} dependence and are filled into the B_0 matrix. The vector potential curl terms lack explicit frequency dependence and are filled into the B_1 matrix. The jump potentials on the self term, even though part of the vector potentials, need to be separated and filled into the B_1 matrix.

Because the PMCHWT case contains no $\sqrt{\omega}$ frequency dependencies, it could be expanded around ω instead. However, in order to keep a general formulation that will hold for multi region problems which may contain a combination of PMCHWT and surface impedance

boundaries, the expansion is still performed around $\sqrt{\omega}$. Results with dielectrics aren't quite as accurate as those for the EFIE. This is probably due to a greater actual frequency dependence than is expressed explicitly for the PMCHWT.

MFIE / CFIE

All of the potentials used by the MFIE are also used by the PMCHWT. This means that once a code has AWE implemented for PMCHWT, it can automatically use AWE on the MFIE. The MFIE is expressed by

$$\hat{\mathbf{n}} \times \mathbf{H}^s(\mathbf{J}) + \hat{\mathbf{n}} \times \mathbf{H}^i = 0, \quad (20)$$

where

$$\mathbf{H}^s = \frac{1}{\mu} \nabla \times \mathbf{A}(\mathbf{J}). \quad (21)$$

However, this leads to a situation where the matrix elements are only dependant upon the curl of \mathbf{A} term that is filled into the frequency independent B_1 matrix. If AWE is applied to this system, it will produce a constant result. That is, AWE will return the same values regardless of frequency because all the derivatives of the B_1 matrix are zero. For this reason, AWE should not be used with the MFIE. Because the derivatives of the AWE matrices contain no useful information, a polynomial fit through a few sampled frequency points will provide a more accurate approximation than AWE.

An AWE formulation for the CFIE has a similar problem. The CFIE is a combination of the EFIE and the MFIE. The components of the AWE matrices from the EFIE will be correct, but only a frequency independent term will arise from the MFIE. This prevents the use of AWE as an efficient method for the CFIE.

Coupled Circuit-EM Formulations: Contacts and Coupled System Matrix

Mixed signal simulation has many applications, including EMC and active antennas. These software codes couple a circuit simulator with a full-wave EM simulator. Very small lumped elements, such as resistors, capacitors, and solid-state devices are modeled using the circuit simulator. The EM simulator handles interconnects, transmission lines, or large printed structures such as on-chip inductors. Note that each of the two pieces improves the functionality of the other component. For example, the EIGER EM simulation is capable of handling simple RLC lumped loads between elements. The circuit simulation tie-in allows for more complex or active loads. Many circuit simulators can handle transmission lines in lumped-parameter form. The addition of full-wave EM allows accurate modeling of the cross talk between transmission lines and accurate loss results for wideband simulations. Since these types of applications are typically broadband in nature, the AWE fast frequency sweep is an important component of the overall simulation package.

The method used to implement coupled systems in EIGER is the contact-connection algorithm. A circuit is attached to a spatially localized surface S_c by enforcing at this contact a modified current-continuity equation, a KCL connection, and a KVL connection from the contact to the circuit node. The conditions enforced are equivalent to saying that the voltage at the EM contact element must be the same as the circuit node it is attached to and that any current flowing out of the circuit node must flow onto the surface of the contact EM element. This is shown in Figure 4.

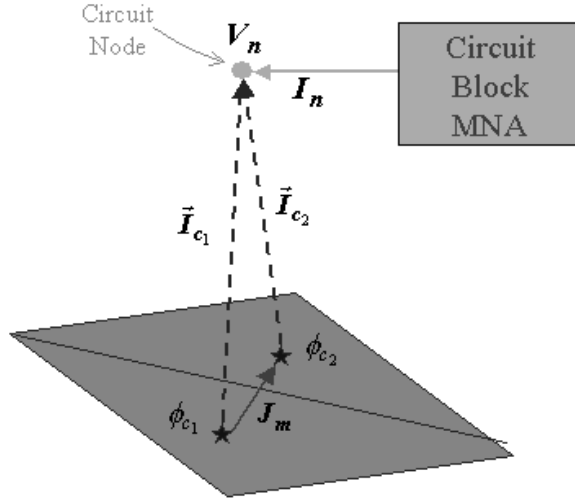


Figure 4: The connection scheme for the contact-circuit algorithm.

On a contact surface S_c , the continuity equation is changed to account for the injecting branch current from the circuit through KCL. This current introduces an additional source term in the continuity equation and thus affects the distribution of both the electromagnetic surface currents and surface charges. Hence, the continuity equation is modified to become

$$\nabla \cdot \mathbf{J} + j\omega\rho = \begin{cases} I_c, & r \in S_c, \\ 0, & \text{otherwise,} \end{cases} \quad (22)$$

where I_c is the contact current.

In addition to adding a current to the EM element, the localized circuit source attached to the contact produces an additional source or sink of charge that alters the scalar potential and the resulting electric field. Because of this additional current, the scalar potentials must be tied to the circuit node voltage V_n . A KVL expression sets the scalar potentials at the equipotential circuit voltage V_n . Finally, the contact current is connected to the circuit by including an addition term I_c to the KCL based circuit equation associated at circuit node n .

The PMCHWT-Circuit formulation, including the connecting KCL and equipotential KVL equations, may be summarized as the following block-matrix equation:

$$\begin{pmatrix} -j\omega(\mathbf{A}_1 + \mathbf{A}_2) - \frac{\nabla}{j\omega}(\phi_1 + \phi_2) & 0 & \mathbf{C}_{12} \\ j\omega(\mathbf{F}_1 + \mathbf{F}_2) + \frac{\nabla}{j\omega}(\psi_1 + \psi_2) & 0 & 0 \\ \mathbf{C}_{21} & 0 & \mathbf{C}_{22} \end{pmatrix} \bullet \begin{bmatrix} \mathbf{J} \\ \mathbf{M} \\ \mathbf{I}_c \end{bmatrix} = - \begin{pmatrix} 0 & -\nabla \times (\frac{\mathbf{F}_1}{\epsilon_1} + \frac{\mathbf{F}_2}{\epsilon_2}) & 0 \\ \nabla \times (\frac{\mathbf{A}_1}{\mu_1} + \frac{\mathbf{A}_2}{\mu_2}) & 0 & 0 \\ 0 & 0 & 0 \end{pmatrix} \bullet \begin{bmatrix} \mathbf{J} \\ \mathbf{M} \\ \mathbf{I}_c \end{bmatrix} + \begin{pmatrix} 0 & 0 \\ 0 & 0 \\ -1 & -1 \end{pmatrix} \bullet \begin{bmatrix} \mathbf{V}_1 \\ \mathbf{V}_2 \end{bmatrix}$$

$$\begin{bmatrix} \mathbf{I}_1 \\ \mathbf{I}_2 \end{bmatrix} = \begin{bmatrix} 0 & 0 & -1 \\ 0 & 0 & -1 \end{bmatrix} \bullet \begin{bmatrix} \mathbf{J} \\ \mathbf{M} \\ \mathbf{I}_c \end{bmatrix} \quad (23)$$

The two-region PMCHWT formulation along with the circuit can be combined into a large system which contains both the MoM matrix and a matrix of modified nodal analysis ($\overline{\text{MNA}}$) circuit equations representing lumped circuit elements:

$$\begin{bmatrix} \overline{\text{EM}} & \overline{\mathbf{X}} \\ \overline{\mathbf{X}}^T & \overline{\text{MNA}} \end{bmatrix} \mathbf{x} = \mathbf{z}, \quad \mathbf{x} = \begin{bmatrix} \mathbf{J}_s \\ \mathbf{ckt} \end{bmatrix}, \quad \mathbf{z} = \begin{bmatrix} \mathbf{b} \\ \mathbf{ckt_ex} \end{bmatrix} \quad (24)$$

Here the matrix $\overline{\mathbf{X}}$ expresses the coupling between the electromagnetic ($\overline{\text{EM}}$) and circuit ($\overline{\text{MNA}}$) parts of the system. Also, \mathbf{ckt} represents the voltages and currents in the circuit part of the system while $\mathbf{ckt_ex}$ is a circuit excitation vector containing voltage and current sources. Finally, \mathbf{x} and \mathbf{z} are composite vectors containing both EM and circuit unknowns, and EM and circuit excitations, respectively.

In order to successfully apply AWE, each piece of this large block matrix must be filled into the appropriate AWE sub-matrix. For the EM block, the only addition is the scalar potential introduced by the contact. Since this is a scalar potential, it has a f^{-1} variation and can be added to the B_0 matrix. The MNA matrix can contain capacitive, resistive, or inductive elements, which should be filled into B_0 , B_1 , or B_3 respectively. The \mathbf{X} blocks, which select the contact nodes which connect to a given circuit node, are filled entirely of 1 or 0. Since the connection between elements and nodes does not change with frequency, these can be filled into the B_1 matrix.

Apart from the filling of the AWE submatrices, there is one more difficulty which can arise with coupled circuit-EM problems. Some of the circuit unknowns will have a solution which is completely independent of frequency. This can occur when the unknowns represent the voltage or current at a voltage divider or a terminal of a source tied to ground. In this case, the Hankel matrix used to solve for the denominator coefficients of the Pade approximation will be singular. To treat this case, a simple test can be performed before attempting to find the denominator coefficients. If all of the derivatives of the solution ($x_1, x_2 \dots x_k$) are zero, the numerator and denominator coefficients of the Pade rational function can be set to

$$[L/M] = \frac{x_0 + 0\tau + 0\tau^2 + \dots + 0\tau^L}{1 + 0\tau + 0\tau^2 + \dots + 0\tau^M} \quad (25)$$

which gives the correct frequency independent value without a singularity.

Coupled Circuit-EM Formulations: N-port representation

The large coupled matrix system can look directly at the impact the two systems have on one another. However, if either the circuit or EM configuration is to remain fixed while the other is changed, it is more efficient to develop a way to separate the two. EIGER uses an N-port representation to do this. The N-port result is a port admittance matrix showing the relation between the voltages and currents at each port for a given frequency. This information can then be incorporated into the circuit model, and used to quickly and accurately evaluate many circuits using the same EM pieces.

The N-port representation is a way to tie the EM matrix to the circuit matrix. It does this by removing the EM unknowns (J) and replacing them with a port analysis based on circuit nodes. The N-port representation is given by

$$Nport = \bar{X}^T \bullet EM \bullet \bar{X}. \quad (26)$$

The X matrix has 1's where circuit unknowns join the EM contacts. The multiplications of EM with X is then equivalent to separately exciting each of the circuit contacts with a unit voltage. The X transpose matrix selects the port currents and voltages for these excitations. The end result is the N-port matrix, which shows the voltage and current at each circuit node for a unit voltage or current applied at any other node.

In order to solve for the N-port representation using AWE, it is expressed as a linear matrix equation with multiple right hand sides. If EM is the number of EM unknowns, N is the number of circuit nodes, then the transformation is shown below

$$\begin{aligned} [Nport]_{N \times N} &= [X]_{N \times EM}^T [M]_{EM \times N} \\ [M]_{EM \times N} &= [Z]_{EM \times EM}^{-1} [X]_{EM \times N} \\ [Z]_{EM \times EM} [M]_{EM \times N} &= [X]_{EM \times N} \end{aligned} \quad (27)$$

Now the intermediate matrix M is the result of a linear matrix system. When each column of M is solved for using the matching column of X, the M matrix can be filled using a multiple right hand side AWE approach. When the N-port approximate solution for a given frequency is desired, the M matrix is first found using the Pade approximations, then multiplied by the X transpose matrix. This increases the cost per approximate frequency by $O(N^2)$ as the number of ports is assumed to be small relative to the number of EM unknowns. While this method does increase the time to get an approximate solution using AWE, it allows for a more versatile output than the coupled circuit-EM solution only. It also reduces the total number of unknowns in the matrix inversion.

Lumped Loads

Lumped loads can be incorporated into an electromagnetic simulation without resorting to a coupled circuit-EM simulation. Implementing them directly into the circuit matrix, when appropriate, results in fewer unknowns than if a coupled formulation is used. Lumped loads are inserted between element edges as shown in Figure 5. They contribute only to the self term in the impedance matrix. Since lumped loads only contribute to the self term, they can be implemented in AWE by modifying the self terms in the B matrices as appropriate.

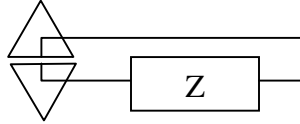


Figure 5. A lumped load connected between two surface elements

Three types of lumped loads are implemented in EIGER. The Z loads, whose impedance does not vary with frequency, series RLC loads, and parallel RLC loads. The Z loads are the easiest to handle in AWE. The impedance value is simply filled into the B_1 matrix. For the series RLC load, the total impedance is given by

$$Z = R + j\omega L + \frac{1}{j\omega C}. \quad (28)$$

This impedance is easily separated by frequency dependence. The resistance is filled into B_1 , the inductance into B_3 and the reciprocal capacitance into B_0 .

Parallel RLC loads are more difficult to implement. The impedance for a parallel load is

$$Z = \frac{1}{\frac{1}{R} + j\omega C + \frac{1}{j\omega L}}. \quad (29)$$

Unfortunately, this equation cannot be split up in terms of frequency components to match the standard AWE process. An attempt was made to approximate the impedance using the equation

$$Z = \frac{B_0}{g} + B_1 + \sqrt{g} B_2 + g B_3. \quad (30)$$

However, this form does not match the actual frequency dependence very well. In fact, in some situations a simple constant approximation is more accurate. The constant approximation is also easier to form, so it is currently used in EIGER. It does not have the same accuracy bandwidth as for the other two types of impedance loads, but can still be more efficient than a sweep without AWE.

7. Results

A number of test cases were run using both EIGER and a Matlab implementation similar to EIGER. These cases were used to test the AWE method as well as refine its operation.

PEC Dipole in free space with delta-gap source

To test the basic EFIE implementation, a strip dipole made of triangles was used. There were 23 unknowns on the dipole and it was fed by a delta-gap source at its center. The dipole dimensions were $39 \text{ cm} \times 1 \text{ cm}$, giving a resonant frequency of about 1.3 GHz. The automated AWE frequency sweep was used and the resulting errors are shown in Figure 6. The error norm of the approximation compared to the exact solution is shown by the diamonds, where each expansion point is shown as a square. It is clear by the clustering of the expansion points near the upper bound that the AWE approximation becomes worse at higher frequencies.

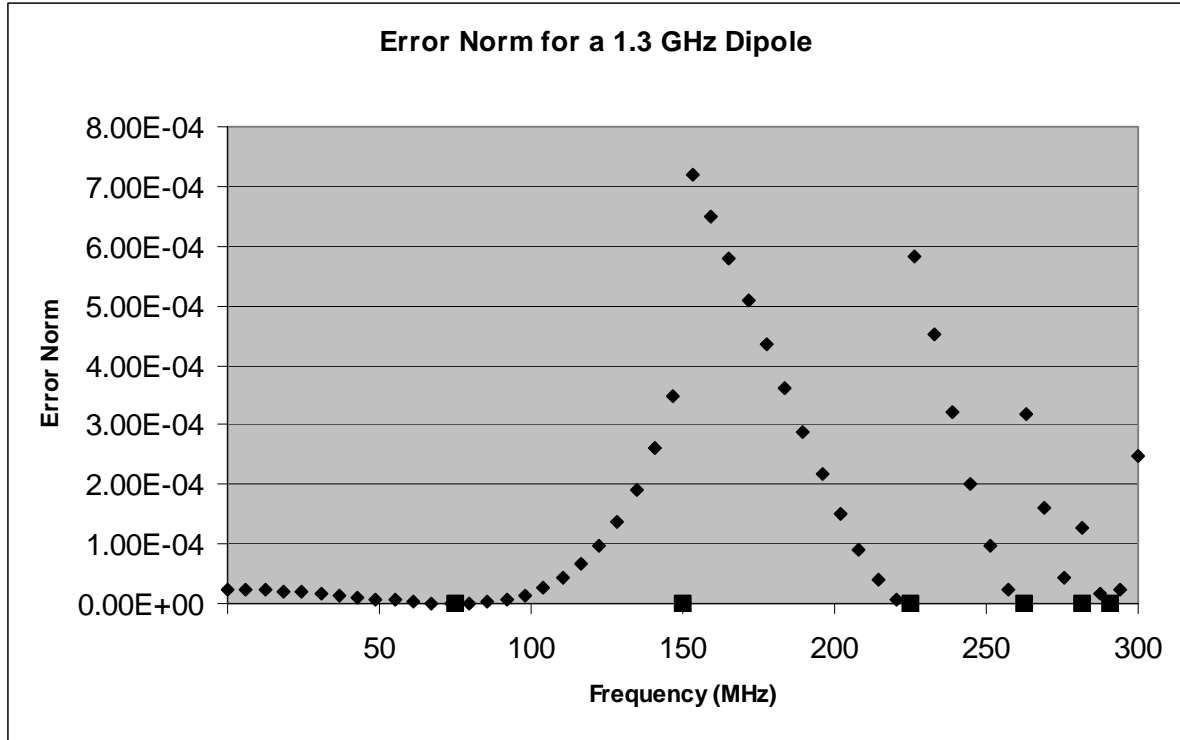


Figure 6. Error norm for a PEC dipole in free space. The blue markers show error of AWE versus exact simulation. The pink points show the expansion frequencies.

As the frequency increases even further, it is apparent that the AWE becomes useless, requiring more expansion points than the desired sampling density. This behavior can be seen in Figure 7. For this dipole, the AWE is only useful up to where the dipole is $1/8$ of a wavelength or so.

The input impedance of the dipole is shown in Figure 8. This plot compares both the exact results and AWE results. It is clear that the AWE shows very good agreement with the exact solution.

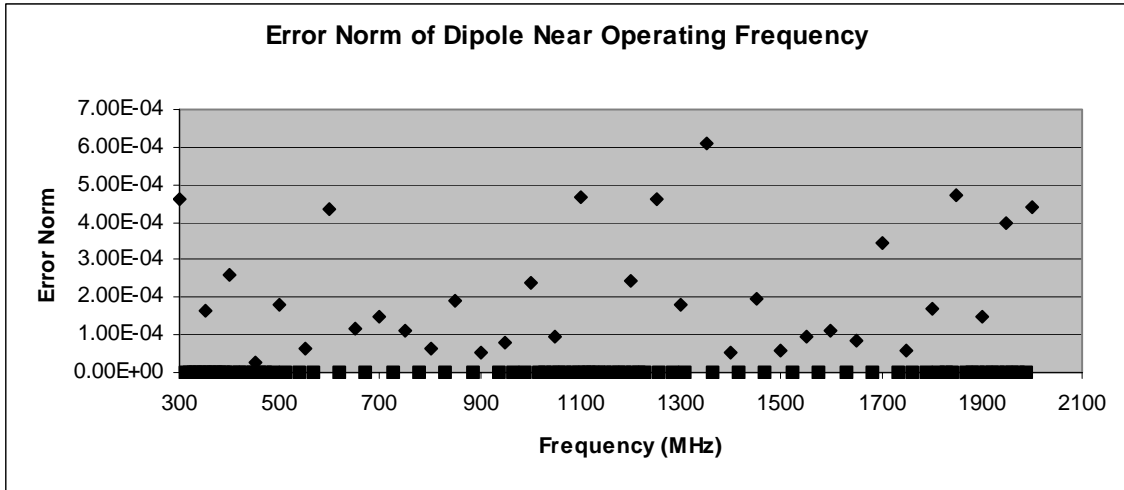


Figure 7. The AWE error norm and expansion points near the operating frequency of 1.3 GHz.

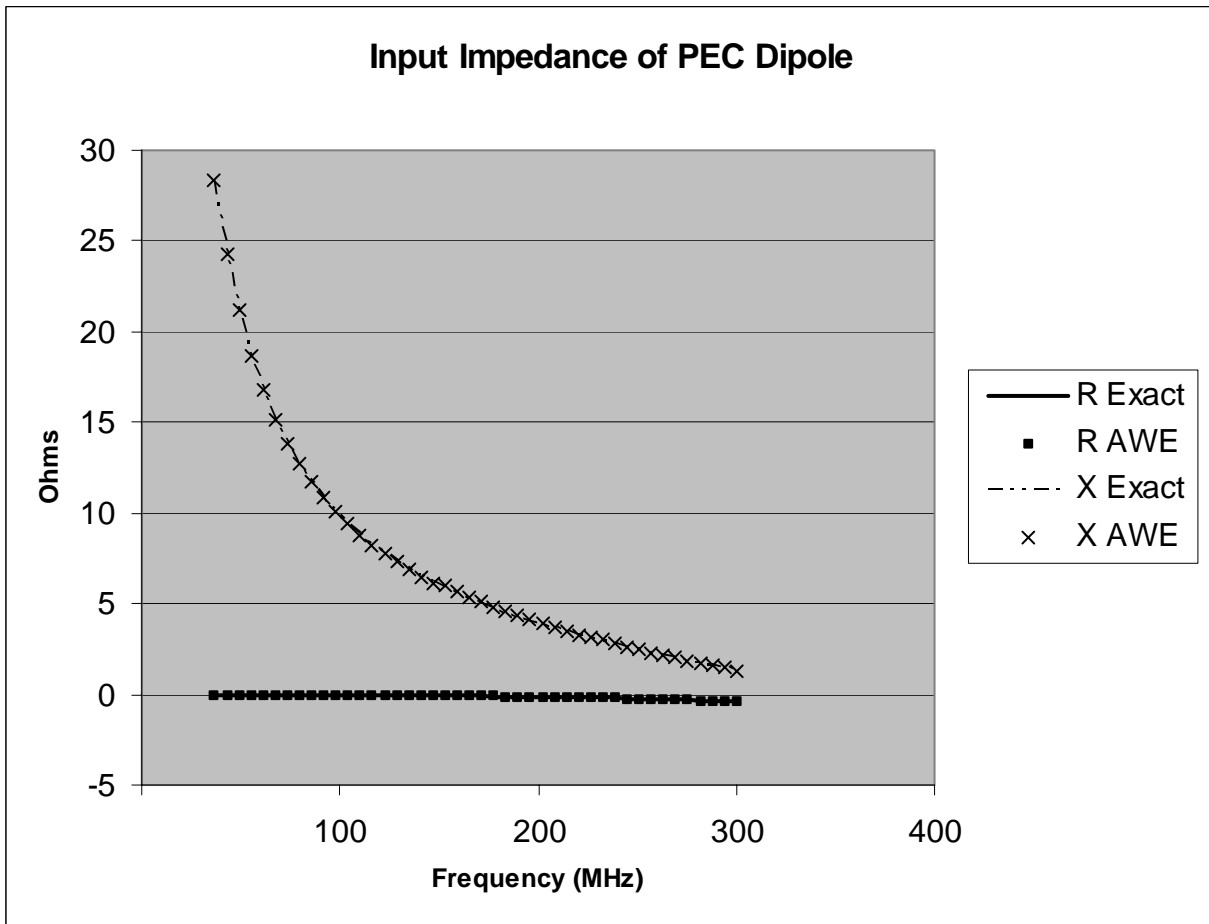


Figure 8. The input resistance and reactance of a PEC dipole. Markers show the AWE approximation, while solid lines show the exact simulated solution.

For the frequency sweep up to 300 MHz, the exact solution took 77.11 seconds, while the AWE sweep completed in 12.4 seconds. This gives an improvement ratio of 6.2. If the exact

solution was needed at more points, the improvement from the AWE would be even more dramatic.

Conducting Dipole in free space with delta-gap source

The same dipole was also simulated using a surface impedance boundary condition. The conductivity used was $5.8E7$, that of copper. Because of a problem with EIGER, the surface load was not added to the center triangle, but was added to all other triangles. The performance of AWE on this dipole was essentially the same as for the dipole in free space. AWE required the same number of frequency points for the expansion and had approximately the same error.

Dielectric Cube

The PMCHW formulation was tested on a simple dielectric cube. The cube was tested with both a delta-gap source and a plane wave excitation. The dielectric cube and the position of the voltage source are shown in Figure 9. The cube is comprised of 12 triangles and has a side length of 10 cm. It was simulated in free space, with the relative permittivity of the cube set to 10.

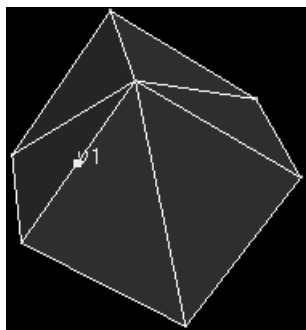


Figure 9. A simple dielectric cube.

A comparison of the AWE error norms from a single frequency expansion point is shown in Figure 10. The voltage source excitation produces the lowest error, while the plane wave source with the correct first two derivatives used in the y vectors has the next lowest error. From this plot, it is clear why the plane wave correction is necessary.

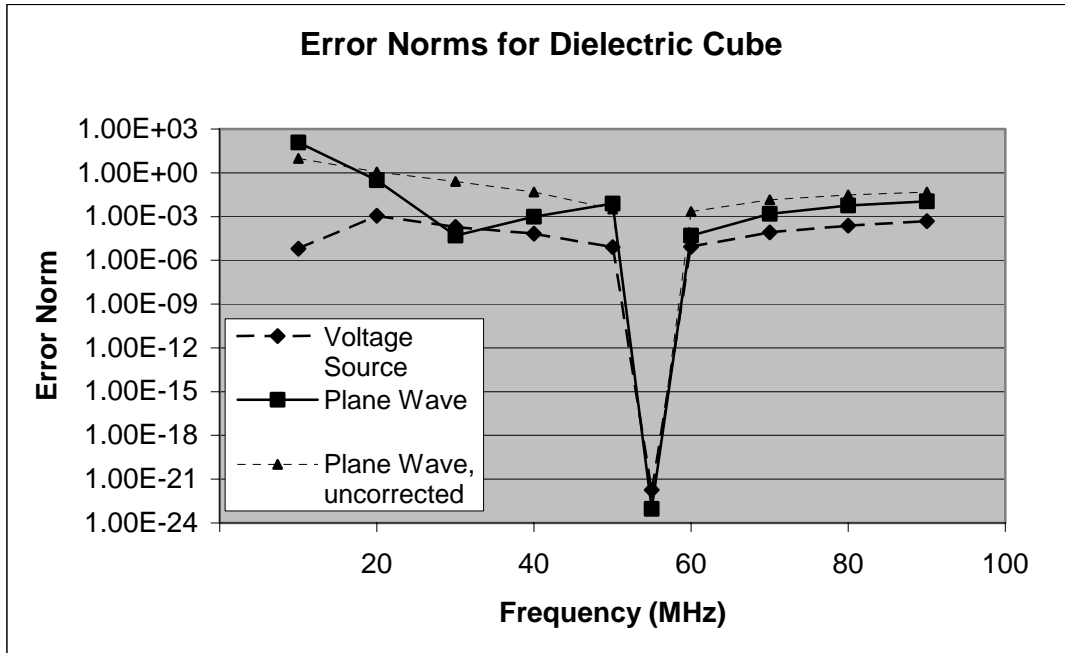


Figure 10. Error results for a simple dielectric cube. The AWE performance is better for voltage sources than for plane waves, although the corrected plane wave form offers some improvement.

Lumped Load Test

The lumped load formulation was tested for a simple ring configuration. The geometry of the ring is shown in Figure 11. The ring is 10 cm on a side and is fed with a voltage source on one side and loaded with a lumped load on the other side. For this structure at low frequencies, the lumped load should dominate current behavior. Therefore, it is a good test of the lumped load formulation.

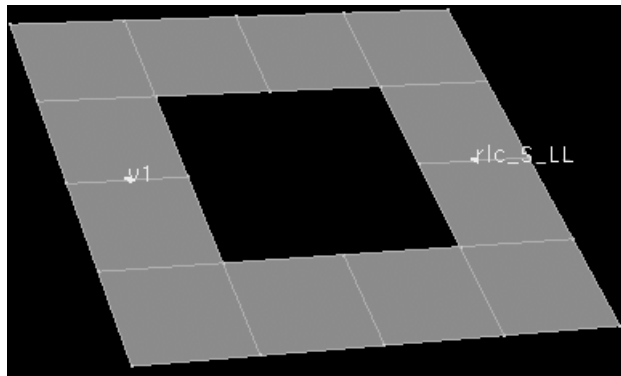


Figure 11. A square ring formed used to test the lumped load formulation. At frequencies where the ring is electrically small, the lumped load should be the dominant factor in controlling surface currents.

The frequency independent Z load was tested first. The load used was $Z = 100 + j200 \Omega$. The error results, shown in Figure 12, show that one AWE point is sufficient to model the structure over a decade.

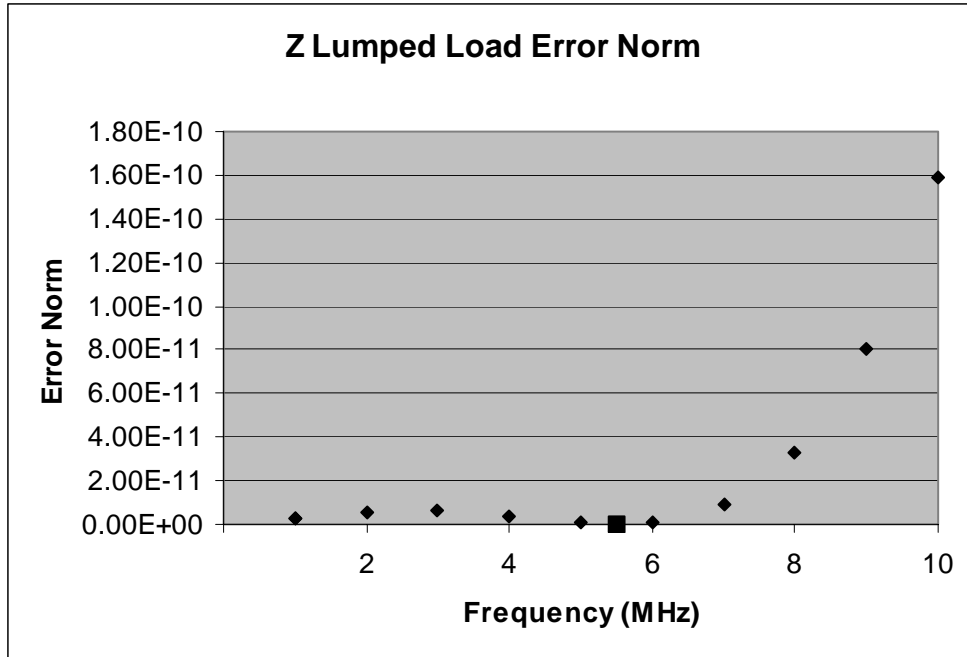


Figure 12. The error norms for a lumped load that is constant with frequency are very low.

A test with a series RLC circuit produced even better results. The RLC circuit was chosen to be resonant at 10 MHz by setting $R = 1000 \Omega$, $L = 1.592E-7 \text{ H}$, $C = 1.592E-7 \text{ F}$. For this case, a single AWE expansion point was suitable to model the problem over three decades. The time for AWE was 3.7 seconds, while the exact method took 58.5 seconds.

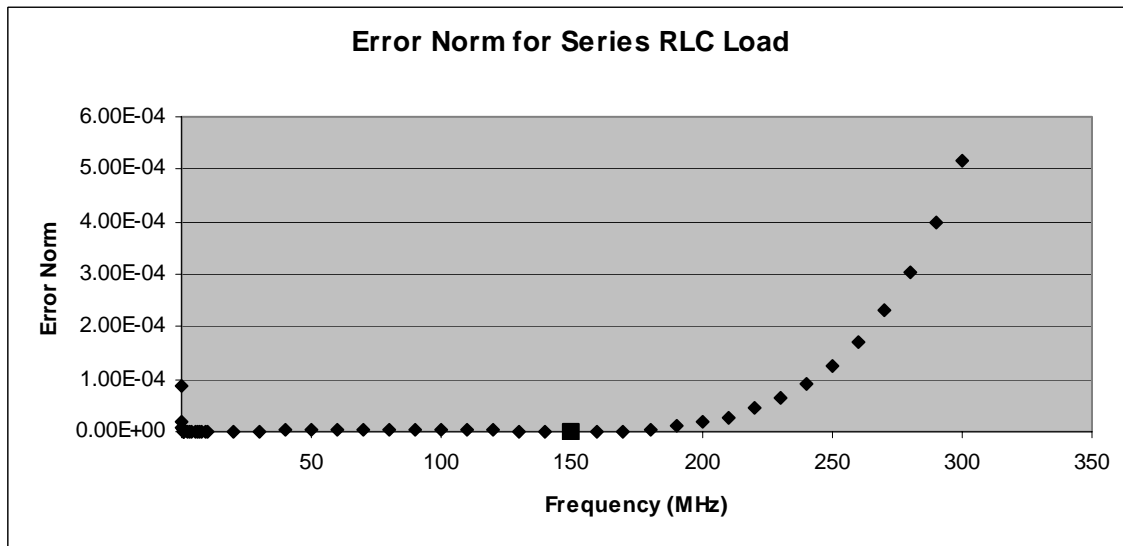


Figure 13. The error performance for an electrically small ring containing a series RLC lumped load.

The RLC parallel lumped load was also tested. Results around resonance were poor, so it was tested above resonance, choosing $L = 1.592E-4 \text{ H}$ and $C = 1.592E-4 \text{ F}$. The parallel load required three expansion points, even though it was not near resonance. Such poor behavior is

expected because the impedance of a parallel RLC circuit cannot be fit correctly into the AWE frequency separation.

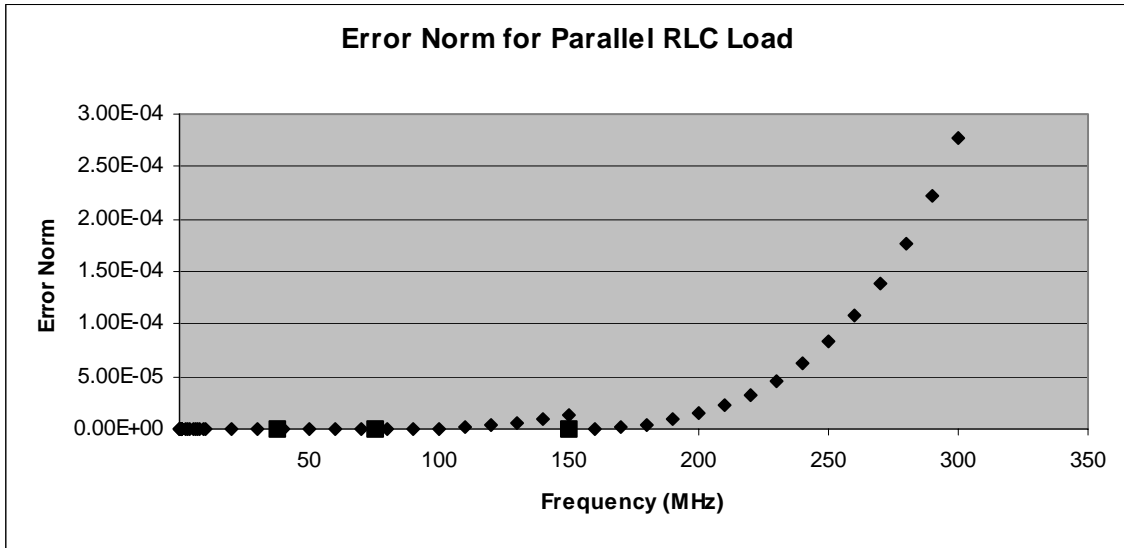


Figure 14. The error norm for an electrically small ring with a parallel RLC load.

Resistive Interconnect

A very simple test of the coupled circuit-EM formulation is a resistive interconnect. The interconnect was modeled using the PMCHWT formulation, with a conductivity of $5.7E8$ mhos on the interior. The dimensions of the interconnect are $1\text{ mm} \times 1\text{ mm} \times 4\text{ mm}$. The interconnect is excited by a circuit voltage source which is connected to contacts on its ends, as shown in Figure 15.

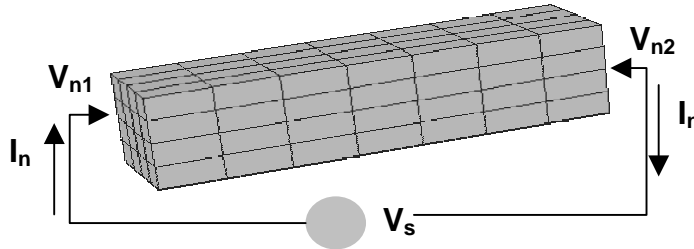


Figure 15. The geometry and circuit definitions for the copper interconnect. The interconnect dimensions are $1\text{ mm} \times 1\text{ mm} \times 4\text{ mm}$. The circuit is connected to both ends by contacts.

The terminal resistance across the interconnect for both the AWE frequency sweep and the standard method in Figure 16. The AWE required 24 minutes, while the exact method required 168 minutes. This test showed that coupled circuit-EM problems can be solved successfully using the AWE method

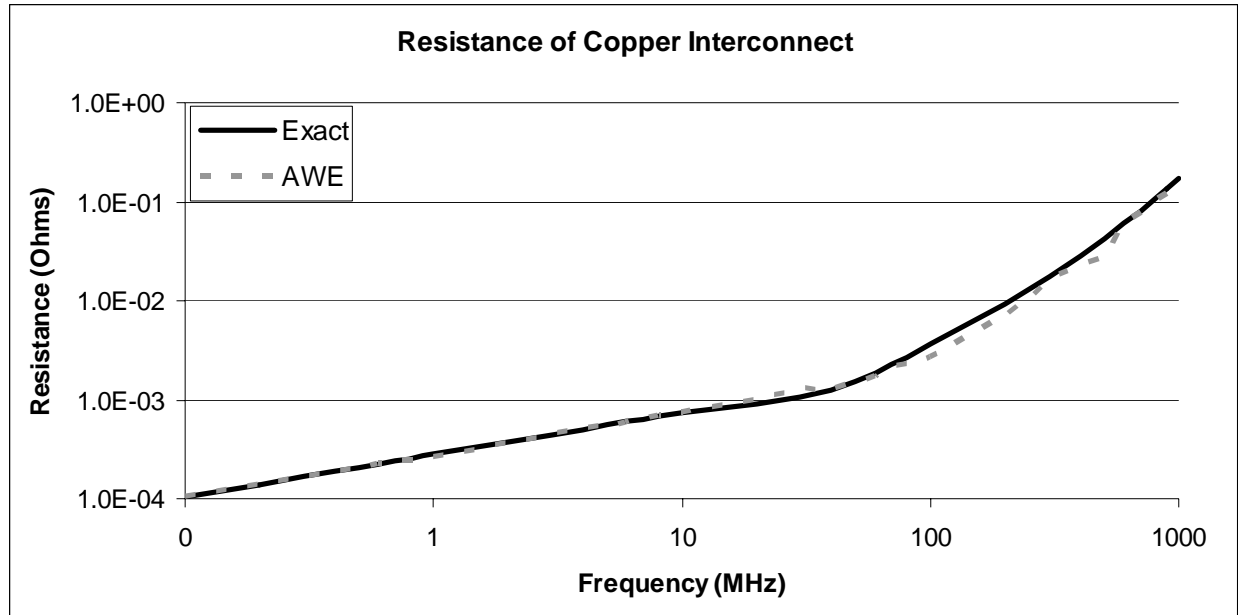


Figure 16. Terminal resistance of the copper interconnect for both the fast and standard method.

8. Conclusion

The Asymptotic Wave Expansion method was developed and applied in the EIGER computational electromagnetic code. The AWE method was expanded to include the PMCHWT dielectric formulation, lumped loads, and coupled circuit-EM problems. A simple adaptive sweep was shown to be effective for some problems. Good results were demonstrated for test problems including resistors and printed circuit dipoles.

9. References

- [1] Jandhyala, V., West, T., "A Fast Frequency Sweep Method for Mixed Electromagnetic and Circuit Simulation", University of Washington Internal Report.
- [2] Baker, George Jr., Essentials of Pade Approximants. Academic Press, New York, NY, 1975.
- [3] Goins, L, Smith, W.T., "Reduced Order Modeling of Thin Wire Scatterers", Proceedings of the IEEE Southeastcon, 1999, pp. 323 - 328.
- [4] Feldmann, P., Freund, R.W., "Efficient Linear Circuit Analysis by Pade Approximation via the Lanczos Process," IEEE Transactions on Computer-Aided Design of Integrated Circuits and Systems, May 1995, pp. 639 – 649.
- [5] Slone, R, Lee, J-F, Lee, R., "Automating Multipoint Galerkin AWE for a FEM Fast Frequency Sweep," IEEE Transactions on Magnetics, March 2002, pp. 637 – 640.
- [6] Chiprout, E, Nakhla, M, "Transient Waveform Estimation of High-Speed MCM Networks Using Complex Frequency Hopping", IEEE Proceedings of the Multi-Chip Module Conference, 1993, pp. 134 – 139.